Iranian Journal of Geophysics, Vol 17 No 3, 2023, Page 77 – 89 (Research Article)
DOI: 10.30499/ijg.2023.364057.1459

Improving runway visual range calculation using an optimized optical parameter

Yashar Rostami[1], Farhang Ahmadi Givi[2*] and Samaneh Sabetghadam[2]

[1]M.Sc. Graduate, Institute of Geophysics, University of Tehran, Tehran, Iran
Technical expert of meteorological organization, Tehran, Iran
[2] Associate Professor, Department of Space Physics, Institute of Geophysics, University of Tehran, Iran

(Received: 01 October 2022, Accepted: 8 March 2023)

Abstract

Visibility deterioration may have negative impacts on aviation safety, particularly in landing and take-off procedures. Beside traditional weather observation methods which are based on human visual estimations, automatic weather observation systems (AWOS) are recently used in airports in order to provide instant measurements of the relevant meteorological parameters. One of the most important sensors is the RVR sensor. In this study, the variability of human visibility and optical instrumental visibility, including the meteorological optical range (MOR) and runway visual range (RVR), along with the probable differences between their values are investigated from December 2019 to February 2020 at Payam Airport, Karaj, Iran.

Results indicate that in different weather conditions, the values of MOR and RVR are predominantly greater than human visibility. In this investigation, MOR is about 99% and 96% more than observed visibility for daytime and nighttime, respectively. The probable reasons for such discrepancies between these two sources of data have argued in this paper. However, to overcome the differences between the two methods, an optimized parameter is introduced as visual optical range (VOR). This parameter simulates human's visibility through MOR to gain the benefits of both methods. Using darkness coefficient, the new parameter depends not only on extinction coefficient but also on sky brightness. The value of 0.07 is proposed for VOR calculation instead of 0.05 in the calculation of MOR. Meanwhile, in the new method, RVR value is also taking the greater values of the Allard's visibility and VOR rather than MOR. Applying this method, it is observed that VOR values align between traditional and instrumental visual ranges. Furthermore, the new method gives more reasonable results considering minimum values of the runway's light intensity over nighttime.

Keywords: Visibility, meteorological optical range (MOR), runway visual range (RVR), Koschmieder's law, Allard's visibility, visual optical range (VOR)

*Corresponding author: ahmadig@ut.ac.ir

1 Introduction

Human visibility is the ability of the eye to detect objects in the surrounding environment. The first visual range data are referred to thousands of years in which mariners have sighted ships, and have made the appropriate entries in their logs, but this mass of miscellaneous information is of little use in predicting of visual range (Duntley, 1948). Thereafter, visibility term has been used to provide a quantitative representation of observation throughout the past decades. Many visibility indices have been proposed to quantify the appearance of a scene (Malm, 1999). However, there was no unified definition of visibility and it was usually referred to as the distance of an object will be just visible (Lee and Shang, 2016). This distance, referred to the ordinary objects against the horizon is called by meteorologists the visibility (Middleton, 1947). It is a function of three variables including: 1) the optical properties of the atmosphere as extinction coefficient, 2) properties of the object and its background, and 3) the adaptation state of the observers' eyes (Malm, 1999). Moreover, two distinctive levels of visibility can be considered in human visual decision processes inclusive of the detection of an object, and its identification (Zege, 1991). Since either detection or identification of an object depends on observer's eyes adaptation, visibility can be defined as a distance where the contrast of the target equals the contrast threshold of the human eye (Horvath, 1981). In fact, this definition is a simple description of the Koschmieder's law (Koschmieder, 1924) that determines the relationship between the apparent luminance contrast of an object against the horizon sky viewed by a distant observer (ICAO, 2005).

Consequently, meteorological daily visibility is defined as the greatest distance at which a black object of suitable dimensions located on the ground can be seen and recognized when observed against the horizon sky during daylight (WMO, 2008). This definition includes all the visibility variables such as color and dimensions of the object, identification concept, sky brightness except observer's eye adaptation. Despite various aspects of visibility definitions, in order to unify them, it can be considered as a function of an atmospheric property called the extinction coefficient (Ex-Co or $\boldsymbol{\sigma}$). This quantity demonstrates the proportion of luminous flux lost by a collimated beam due to both absorption and scattering while travelling the length of a unit distance in the atmosphere (WMO, 2008). According to Eq. (1), $\boldsymbol{\sigma}$ can be shown as two separate terms of absorption and scattering (Douglas and Booker, 1977):

$$\boldsymbol{\sigma} = \boldsymbol{\sigma}_{\text{absorption}} + \boldsymbol{\sigma}_{\text{scattering}} \quad (1)$$

Atmospheric pollutants, including aerosols and gases may cause a visible reduction by absorbing or scattering of visible light. Both gases and particles scatter and absorb radiation and contribute to the light extinction coefficient of the atmosphere. Scattering depends on the ratio of the particle to the wavelength of the incident light (Liou, 2002). In the atmosphere, the particles responsible for scattering, cover the sizes from gas molecules to large particles. When particles are much smaller than the incident wavelength, the scattering is called Rayleigh scattering. For particles whose sizes are comparable to or larger than the wavelength, the scattering is customarily referred to as Mie scattering (Stuke, 2016). Since visibility has reverse relation with Ex-Co parameter, in many of the visibility estimation methods such as instrumental measurements, including transmissometer and scatter-meter and digital image processing technique, the value of extinction coefficient is taken into account in order to obtain visibility.

The results of previous investigations

of the visual ranges indicated that during daylight, the value of the visibility, which is reported by human observer is about 15% higher than the instrumental measurements (WMO, 1990), while the results of recent experiments are fairly contrary to the former results. In other words, investigations in recent decades demonstrate lower values for observer's visibility compared with different instrumental measurements such as transmissometer (Jenamani and Tyagi, 2011), scatter-meter (Cornick, 1993; Matsuzawa and Takechi, 2012) and image processing (Kim, 2018). Results of using digital image processing technique over the city of Tehran showed that extinction coefficients, estimated by human observers, were more than those of the digital image processing method (Sabetghadam et al., 2014).

The purpose of the current study is to examine the variability of both traditional and instrumental visibility along with their differences. The main goal is to do an extensive analysis of the deficiencies of each method. However, we cannot determine that which method is more precise quantitively. After comparison and identification of deficiencies of each method, to partially overcome the drawbacks, an extended and optimized parameter is introduced as visual optical range (VOR) to estimate the visibility using the benefits of both methods.

The structure of this paper is as follows. Section 2 presents the data sets and methodology used in this research. The results of investigation of traditional and instrumental visibility together with their deficiencies are given in section 3. The new optimized method and its evaluation are also described in this section. Finally, the concluding remarks are presented in section 4.

2 Materials and methods

For aeronautical purposes, visibility is determined as the greatest value between the following two estimations: a) the distance in which a black object of suitable dimensions can be seen and recognized against a bright background, b) the distance in which lights in the vicinity of 1000 candelas can be seen and identified against an unlit background (ICAO, 2005). In this study, these two categories are denoted as V_a and V_b, respectively. The greater value between V_a and V_b can be considered as visual range (V_R) and defined as the maximum horizontal distance in which a given light source or object is just visible under particular conditions of background luminance. In order to determine visibility at airports, landmarks around the airport have been implemented on visibility chart in which the distance of the farthest visible landmark detected by the observer is reported as observational visibility value.

Beside the above-mentioned traditional method for the estimation of visibility, optical sensors including transmissometer and scatter-meter are usually applied to measure visibility at airports. The results of the first WMO inter-comparison of visibility measurement methods indicate that the performance of scatter-meters are generally less accurate than transmissometers for the determination of low visibilities (WMO, 1990). To determine visibility values via optical transmissometers and scatter-meters, the value of extinction coefficient should be measured. Bouguer-Lambert's law (1729) describes how luminous flux decreases from F_0 to F when the light travels a bl distance in the atmosphere. Eq. (2) satisfies the condition of contrast (WMO, 2008):

$$F = F_0 e^{-\sigma bl} \Leftrightarrow C = C_0 e^{-\sigma bl} \Leftrightarrow I = I_0 e^{-\sigma bl} \quad (2)$$

where C is the apparent contrast of an object seen from a distance and C_0 is its inherent contrast. I_0 is the light intensity emitted from the transmitter to the receiver in optical transmissometer instruments, I is the light intensity measured by the receiver and bl is the distance between transmitter and receiver (Vaisala,

2011). Koschmieder's law which is used for human visual range estimations, describes that target will be visible on condition that the ratio of (C/C_0) be greater than 0.02 (WMO, 2008). Hence, Koschmieder's law can be obtained after replacing (C/C_0) by the value of 0.02 in Eq. (2) and then taking mathematical ln operator from the equation (Middleton, 1952). Thus, as shown in Eq. (3), the Koschmieder visibility is defined only as a function of $\boldsymbol{\sigma}$:

$$V_k = 3.912 / \sigma \quad (3)$$

Visibility measurement using a transmissometer is based on the meteorological optical range (MOR) calculation that is defined as the length of the path in the atmosphere required to reduce the luminous flux in a collimated beam from an incandescent lamp, at a color temperature of 2700 K, to 0.05 of its original value (ICAO, 2005). Therefore, MOR can be obtained after replacing (I/I_0) by the value of 0.05 in Eq. (2) (WMO, 2008). More investigations show that the value of 0.05 is more realistic than the value of 0.02, which is used in the Koschmieder equation (Biral, 2010). MOR is defined as:

$$MOR = 3 / \sigma \quad (4)$$

The other important visibility value, known as the Allard's visibility (V_A), is calculated through Allard's law (Allard, 1978) using the following equation:

$$E_T = I_{in} \frac{e^{-\sigma V_A}}{V_A^{\,2}} \quad (5)$$

where E_T and I_{in} are the illumination threshold and the runway light intensity, respectively. The greater value between MOR and V_A is reported as runway visual range (RVR) (ICAO, 2005).

In order to investigate the probable differences between the MOR, RVR and the observational visibility, this study is conducted during December 2019 to February 2020 at Payam Airport, Karaj, Iran. Considering the geographical location of the Payam Airport (35° 45′ 50″ N, 50° 50″ 25″ E), it is expected that various weather phenomena would occur within this period. Table 1 displays the list of different weather conditions occurred in the study period. It indicates the number of days that each weather phenomena occurred during December 2019 to February 2020. It should be mentioned that all the weather conditions have been examined and visibility values obtained from the above methods as well as the new method introduced in the paper and then have been compared, but only a few cases are presented here.

Table 1. Number of daily weather phenomena occurred during December 2019 to February 2020. No cloud and visibility of more than 10 km are considered as CAVOK weather condition.

weather	CAVOK	Cloudy	haze	mist	drizzle	rain	snow	fog
Days	29	36	53	43	2	9	10	15

At this airport, like other airports, landmarks around the airport have been implemented on visibility chart in which the distance of the farthest visible landmark detected by the observer is reported as observational visibility value. Alternatively, an optical transmissometer sensor, equipped with a forward-scattermeter and a background luminance sensor, is used to measure MOR and sky brightness. The data intervals synchronized with Payam METeorological Aerodrome Report (METAR) start from 10:30 local time. The MOR values with a limitation of 15000 meters were generated

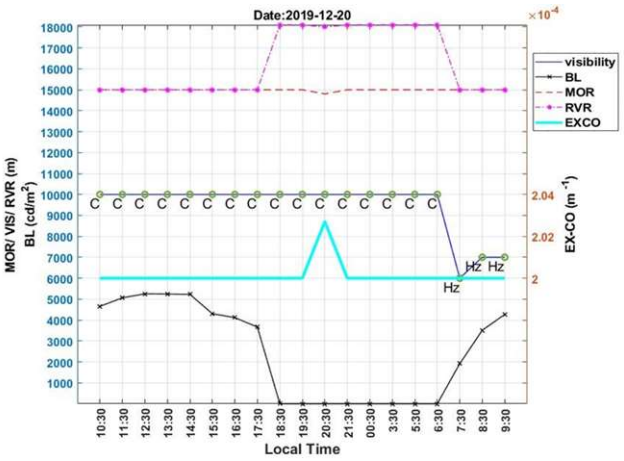

Figure 1. Differences of visual ranges for 20th December 2019. Horizontal axis is local time. Left and right vertical axes represent visual ranges along with BL and Ex-Co, respectively. In this figure, background luminance (BL) is the bottom line. Continuous thick line and coded line are Ex-Co and observer's visibility, respectively. MOR and RVR are dotted lines.

through the sensor, but due to the low level of RVR limitation (values greater than 2000 meter reported as P2000) (ICAO, 2004), it has been taken into account by ICAO (International Civil Aviation Organization) calculation rules with no limitations for values greater than 2000 meter. To reach this, first, the values of illumination threshold (E_T) are determined through Eq. (6). Substituting E_T value into Eq. (5) gives V_A (ICAO, 2004):

$$\log^{ET} = 0.57\log^{ET} + 0.05\log^{BL^2} - 6.66 \quad (6)$$

where BL is the background luminance measured by BL sensor. Then, the greater value between V_A and MOR is considered as the estimated RVR. Also, according to the recommendation of the ICAO, this estimated value by considering Table 2 steps should be rounded down to the nearest lower step in reporting the scale of RVR (ICAO, 2004). Finally, a graph is drawn for each day of the study period. Since it is likely to have simultaneously several reports of present weather code, these data are converted to simple codes as shown in Table 3.

3 Results and discussions

Figure. 1 shows the variation of visibility values achieved by observer and optical sensors for 20th December 2019 in predominant CAVOK weather condition. In this figure, background luminance (BL) indicates the sky brightness and decreases to the value of 2 during the nighttime (Vaisala, 2011). Referring to Figure. 1, MOR and consequently RVR values are highly greater than observer's visibility. This is generally true for all other similar weather conditions within the study period which are not shown for brevity. In this regard, it should be noted that the Koschmieder's law, which is used to estimate observer's visibility, is only applicable to very limited conditions (i.e., the black targets should be viewed against the horizontal sky in homogeneous atmosphere) (Horvath, 1981), while in the Payam Airport some of the landmarks are not black. Thus, utilizing bright targets as landmarks can lead to reduction of observer's visibility.

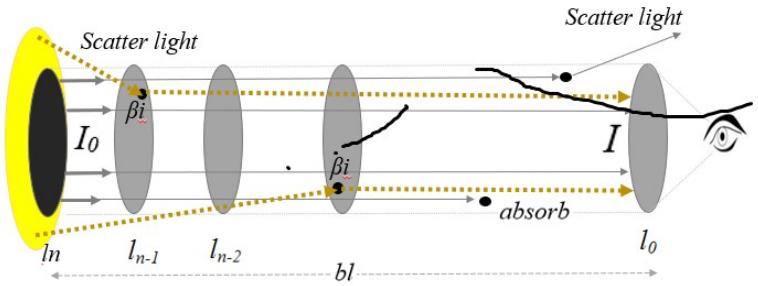

Figure 2. Schematic of lights received by the human eye from the target and its background after traveling bl distance in the atmosphere. βi's are the symbols of atmospheric particles that lead to scattering and interfering of background lights (dotted lines) with the target lights (continues lines).

Table 2. Ranges and resolutions for RVR information included in the meteorological reports (ICAO, 2005)

Element	Range	Resolution
RVR	0-400	25
	400-800	50
	800-2000	100

Table 3. Present weather codes used in this study

Present weather	Code	Present weather	Code
CAVOK	C	Haze	Hz
1/8 cloud	1	Mist	Br
2/8 cloud	2	Drizzle	Dz
3/8 cloud	3	Rain	Ra
4/8 cloud	4	Fog	Fg
5/8 cloud	5	Snow	Sn
6/8 cloud	6	Sand	Sa
7/8 cloud	7	Dust	Du
8/8 cloud (overcast)	8	Not Recording data	N

According to Eq. (2), the other probable cause of the difference between the visibility ranges can be due to the fact that in transmissometer optical sensors, only the ratio of main light source intensities is calculated and background lights are filtered by the receiver but in reality, as shown in Figure. 2, background lights interfere with target lights and cause the human visibility range to reduce. Hence, it seems that the amount of 0.05 in Eq. (4) is not realistic anymore. The amount of missing background lights can be taken into account as an integral term in Eq. (7) in which the inner integral denotes all atmospheric particles on an imaginary disc that has been located in the path of the human visual range. The outdoor integral is the sum of all discs:

$$I = I_0 e^{-\sigma bl} + \int_{bl}\int_{n} \beta_i e^{-\sigma l} didl \qquad (7)$$

Moreover, as seen in Figure. 1, during the sunrise (between 6:30 and 7:30 A.M.), observer's visibility has been decreased from 10 km to 6 km, while sensor data do not show any changes. This is true for many other cases. In order to explain more in detail about the differences, a schematic diagram has been devised by the authors (Figure. 3). This diagram demonstrates changes in visual ranges

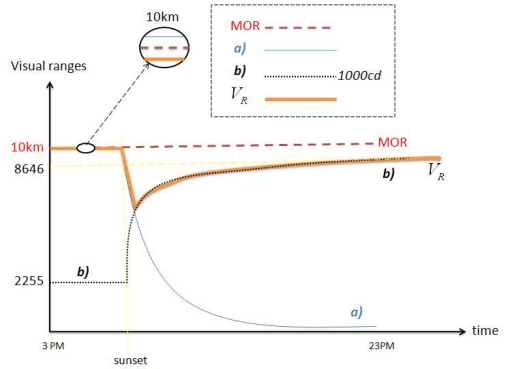

Figure 3. Schematic relationships between visual ranges and sky brightness in a normal day and normal night. The values of 2255 and 8646 for V_b are extracted from ICAO (2005) to have vision of lights with 1000 candela vicinity for daytime and nighttime, respectively. It should be noted that these values can be obtained through the Allard's law (Eq. 5), while there is no equation for V_a calculation.

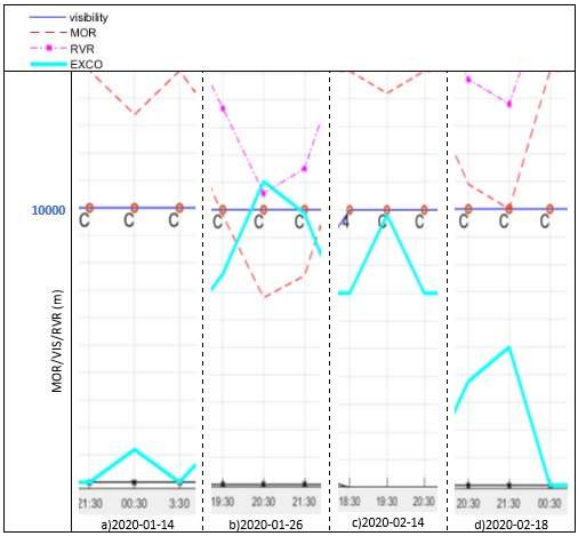

Figure 4. Variations of visual ranges at nighttime for four different cases. Horizontal axis shows a part of nighttime and vertical axis denotes visual ranges. Constant coded line (10 km) and continuous thick line are observer's visibility and Ex-Co, respectively. MOR and RVR are dotted lines. Despite 10 km constant observer's visibility, other lines including Ex-Co, MOR and consequently, RVR are partly changed.

during a normal day and night. As aforementioned, MOR is only derived from Ex-Co and not affected by sky brightness; thus, in the absence of weather phenomena, it remains constant in time. Also, in this weather condition, V_a and V_b are only driven by sky brightness, so after sunset, V_a starts to decrease while V_b increases. Consequently, human visibility (V_R), which is greater than these two parameters is minimized. As a result, in sunset and sunrise times, MOR is greater than V_R and their difference is maximized. Additionally, if weather phenomena occur during the day, even though both MOR and V_R decrease, because of brightness reduction, the difference between MOR and V_R will increase. Therefore, MOR may not represent real visibility when there is high variation of sky brightness.

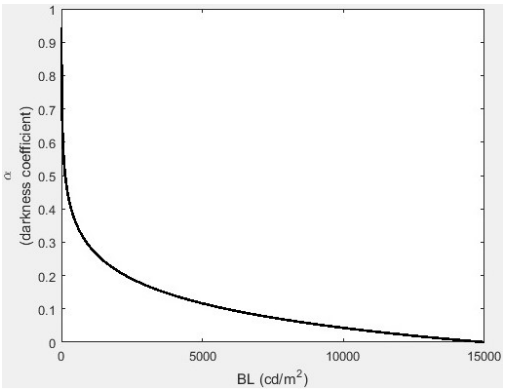

Figure 5. Relation between darkness coefficient and instant background luminance.

Beside the problems of the above optical sensors, they have some advantages. By way of illustration, due to the lack of nighttime standard visibility charts, sometimes observers are not able to detect visibility variations precisely. For instance, although Ex-Co values are increased around 20:30 local time (as shown in Figure. 1), the observer's visibility is constant. Figure. 4 displays visual ranges for four different cases to examine the changes over the nighttime. In all the cases, Ex-Co values and consequently, MOR and RVR are altered during the nighttime while the observer's visibility is constant at 10 km.

In order to cover the aforementioned imperfections of observational visibility and instrumental visual ranges, first a new parameter is introduced to estimate V_a through the instrumental data output. Since the new parameter should be a function of sky brightness, precise measurements of background luminance data are utilized to obtain sky brightness variation. Then, by assuming logarithmic variations of the light proportion, inspired from Eq. (2), sky darkness coefficient (α) is defined by the authors as:

$$\alpha = k.Ln(\frac{BL_{measured}}{BL_{\max}}) \quad (8)$$

where BL_{max} is the maximum brightness in a bright day and $BL_{measured}$ is an instant measurement. The maximum value in the measurement of BL which demonstrates sky brightness, generally depends on the latitude of the station. Therefore, BL_{max} in the Payam Airport is practically around 15000. In order to determine coefficient k in Eq. (8), it can be taken into consideration that during the night, when the critical value of $BL_{measured}$ is around 2, the darkness coefficient α reaches 1 and we get:

$$\alpha = (-0.106)Ln(\frac{BL_{measure}}{BL_{\max}}) \quad (9)$$

Figure. 5 shows the relation between the darkness coefficient and instant background luminance that obtained applying Eq. (9). During the night, when BL is close to zero, darkness coefficient reaches 1, while during bright day, this coefficient approaches 0. Logarithmic changes for BL variations are also shown in Figure. 5. Since α is proposed as the sky darkness coefficient, the term (1-α) would be the sky brightness coefficient and visual optical range (VOR) can be thus given as:

$$VOR = (1-\alpha)\times(2.66/\sigma) \quad (10)$$

or by applying Eq. (4):

$$VOR = (1-\alpha)\times(2.66/3)\times MOR$$

In order to recover the background lights filtered out by the sensor, the threshold value of 0.07 has been used in Eq. (10) rather than the value of 0.05 in Eq. (4). In fact, VOR estimates V_a; ultimately, RVR_{new} is taken to be the greatest value between the Allard's visibility and

VOR instead of MOR.

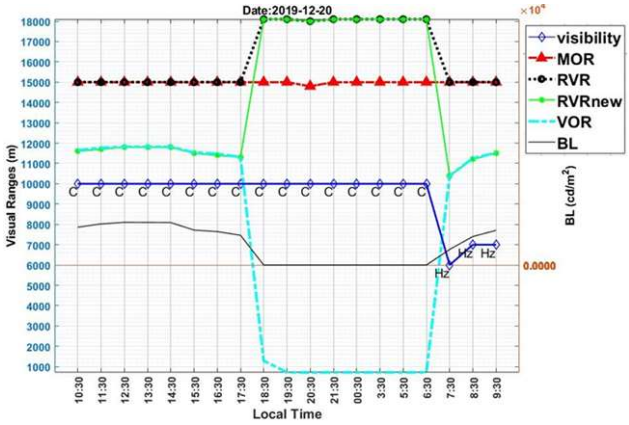

Figure 6. The modified version of Figure. 1 concerning visual ranges for the 20th December 2019. The horizontal axis is local time. Left and right vertical axes represent values of visual ranges and BL, respectively. Lines with different shapes are introduced in the box at the upper right of the figure.

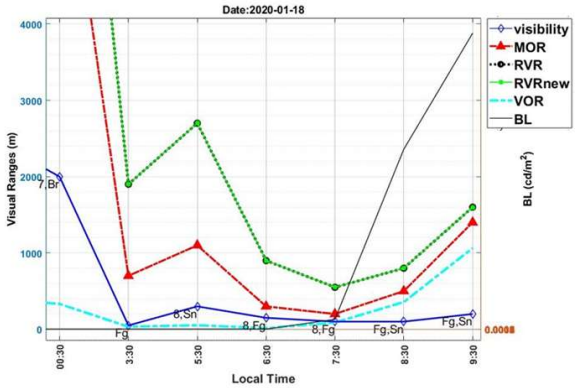

Figure 7. Differences of visual ranges in a foggy and snow weather condition.

Based on the newly proposed Eq. (10), values of the VOR and RVR_{new} are determined and the results are added to Figure. 1 to get Figure. 6. Over the daytime, from 10:30 to 17:30 local time, VOR has values between MOR and observer's visibility. At this time, VOR and RVR_{new} have the same values. After the sunset, VOR like V_a in Figure. 3 falls rapidly due to the brightness reduction, and then the Allard's visibility becomes greater than VOR. Over the nighttime, RVR_{new} values follow the Allard's visibility. During the sunrise between 6:30 and 7:30, VOR increases rapidly as its value becomes greater than the Allard's visibility; hence, RVR_{new} follows the VOR value again. Ultimately, as shown, during sunset and sunrise, like the effect of brightness on the observer's visibility, the values of RVR_{new} are minimized.

As aforementioned, Figure. 6 presents a CAVOK weather condition, which is an example of similar weather conditions examined within the study period. Thus, all the visual ranges are above 2000m, thereby not being of importance for aviation safety. As shown in Figure. 7, we investigate another case concerning a deteriorated visibility condition which is critical for aviation. Figure. 7 displays the variability of visual ranges for 18th January 2020 in a foggy and snowy weather condition starting from 3:30 local time.

Referring to the figure, after sunrise at 7:30 A.M., VOR value is located between MOR and

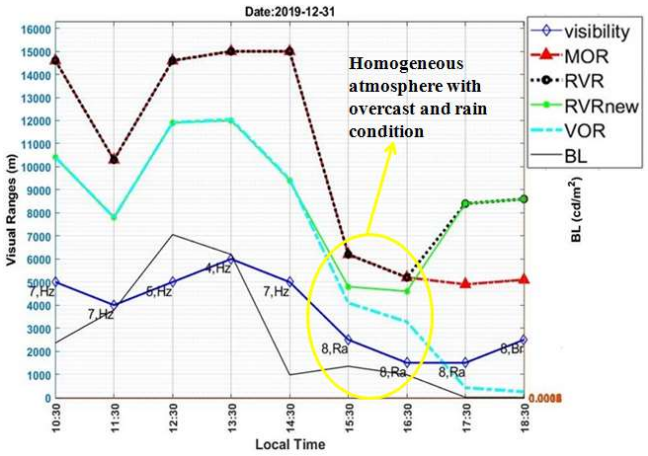

Figure 8. Comparison of different visual ranges for a homogeneous atmosphere started at 15:30 on 31th December 2019.

observer's visibility and both MOR and VOR values have increasing trends, while observer's visibility remains nearly constant at low value which is likely due to the observer's task stress.

Furthermore, it should be noted that transmissometer optical sensors cover only small samples of the atmosphere with maximum distance of 30 meters (Vaisala, 2011), thereby not being representative of the whole area condition. On the other hand, human observation is based on an overview that covers a large volume of the atmosphere but with other limitations. For instance, if an observer is located in a foggy weather with a visibility of 300 m, visibility conditions beyond the distance of 300 m would be fuzzy (Meteo France, 2020). Therefore, investigation of a case concerning a homogeneous atmosphere can provide a better assessment of the results for our purposes.

The comparison of the daytime visual ranges for 31th December 2019 as a case of homogeneous atmosphere is illustrated in Figure. 8. At 15:30 local time, during the occurrence of overcast and frontal rain, VOR was fairly between the values of MOR and observer's visibility. After 16:30, the decrease of sky brightness led to the VOR deterioration. As a whole, during daytime and in all the different weather conditions examined here, the results of the new method are getting closer to reality than the existing methods.

Beside the improvement in the calculation of visual range by removing the cause of errors, the newly defined VOR has an important role in upgrading the estimation of RVR over the nighttime. During the nighttime with low values of runway light intensity, estimation of RVR as the greater value between MOR and Allard`s visibility may lead to a systematic error. Sample values of nighttime MOR and V_A along with different $\boldsymbol{\sigma}$ values and runway light intensity are compared in Table 4 (ICAO, 2005). Assuming the minimum value of 2 for $BL_{measured}$ in Eq. (9), α is obtained about 0.95 at nighttime. Then, using Eq. (10), VOR for different values of MOR was calculated (Table 4). As aforementioned, the greater value between MOR and V_A is reported as RVR. At nighttime, RVR directly depends on the runway light intensity and it is expected that V_A will be reported as RVR. But referring to Table 4 (cells denoted by "*"), MOR is greater than V_A,

and is recorded as RVR. Here, although a wrong value is recorded as RVR, both MOR and V_A are greater than 2000 m, thereby not being an important problem in application. However, in the cells denoted by "**" in Table 4, V_A value is less than 2000 m, hence an important problem when MOR is incorrectly recorded instead of V_A. In order to get a better point of view, it can be taken into consideration a nighttime with 10 km for MOR and runway lights switched off ($I_{in} \simeq 0$). This means that V_A is close to zero; thus real RVR is also zero, while MOR is greater than V_A. Now, if MOR is reported as RVR value, it might result in a very dangerous issue. A part of this problem could be solved by applying the modified VOR value instead of MOR. At nighttime, by decreasing the light intensity and consequently V_A, VOR values remain less than the Allard's visibility as well. Therefore, at nighttime even by decreasing runway light intensity, the Allard's visibility is greater than VOR and recorded as RVR_{new}. This points out the distinct advantage of VOR over MOR.

Table 4. MOR and VOR for different values of $\boldsymbol{\sigma}$ along with V_A values during the nighttime. V_A values are determined using the visual thresholds of illumination (E_T) equal to 10^{-6} lx and different values of runway light intensity (I_{in}). See text for more details.

MOR (m)	10000	3000	1000	300	100	30
VOR (m) $\alpha \approx 1$	480	144	48	14	5	1.5
σ(m-1)	0.0003	0.001	0.003	0.01	0.03	0.1
Iin(cd)	V_A values based on: I_{in}, σ and E_T (at night$\simeq 10^{-6}$)					
10000	13400	5722	2468	935	373	133
1000	*8646	4090	1881	749	309	113
100	*4839	*2653	1340	572	247	93
10	*2255	**1469	**865	409	188	75

4 Concluding remarks

Visibility deterioration may have negative impacts on aviation safety, especially during take-off and landing procedures. Beside traditional weather observation methods which are based on human estimations, automatic weather observation systems (AWOS) are recently used in airports in order to provide accurate instant measurements of the relevant meteorological parameters. One of the most important sensors, which eventuates two essential meteorological parameters inclusive of the meteorological optical range (MOR) and runway visual range (RVR), is the RVR sensor. Although the results of some previous studies indicated that observer estimations were about 15% higher than instrumental measurements, the results of recent experiments are fairly contrary to the former studies. Therefore, in this study the variability of both traditional and instrumental visual ranges, and their differences are investigated. The data include the present weather code and visibility from human observation as well as the MOR values provided from AWOS and RVR calculations during December 2019 to February 2020 at Payam Airport, Karaj, Iran. Examination of differences between observational visibilities and optical measurements reveals both following advantages and drawbacks of each method. Results indicate that optical sensors precisely detect any instant changes of Ex-Co in small samples of the atmosphere. However, eliminating background lights in transmissometer can lead to visibility values greater than those in reality. Therefore, it seems that the threshold value of 0.05 is not accurate and realistic in the MOR calculation. Furthermore, it is found that high variations of sky brightness may have influence on the observer's visibility, while MOR only depends on the Ex-Co

parameter and thereby not representing real visibility in high variation of brightness situation. Although, as a merit of observational visibility, human observation is rapidly influenced by brightness variations, it is not possible to detect small changes of visibility during nighttime. Moreover, lack of suitable black objects around the airport and using bright objects as landmarks can lead to reduction of visibility report.

In order to overcome the deficiencies in observational visibilities and optical visibility measurements, a new parameter has been introduced by the authors as visual optical range (VOR). This new parameter, depends not only on Ex-Co but also on sky brightness. Also, efforts have been made to compensate background lights which are filtered by the optical sensor. In this regard, the liminal value of 0.07 is proposed in VOR calculation instead of 0.05 in the calculation of MOR. In general, the use of new proposed optical parameter shows two distinct benefits. First, the results of visibility estimation applying this parameter are more realistic than those obtained from other methods. In all the weather conditions examined in this study, during the daytime, VOR has the value between MOR and observer's visibility, which is the same value as RVR_{new}, but during the nighttime, VOR falls rapidly due to the brightness reduction while RVR_{new} values follow the Allard's visibility. Second, using the new optical parameter improves the estimation of visibility during the nighttime considering minimum values of runway light intensity. At night, RVR depends not only on MOR but also on the runway light intensity. Therefore, applying the modified VOR value instead of MOR, the Allard's visibility is recorded as RVR_{new} which points out a distinct advantage of VOR over MOR. However, since this study was conducted over a specific region, it is needed to evaluate the proposed optical parameter in other regions and weather conditions.

References

Biral, 2010, Operation and Maintenance Manual for the VPF-730. Combined Present Weather Sensor & VPF-710 Visibility Sensor: Biral, 79 pp.

Cornick, J. C., 1993, A comparison of ceiling and visibility observation for NWS manned observation sites and ASOS sites: Colorado State University, Report, 71 pp.

Douglas, C. A., and Booker, R. L., 1977, Visual Range: Concepts, Instrumental Determination, and Aviation Applications: US Department of Commerce, National Bureau of Standards, 373 pp.

Duntley, S. Q., 1948, The visibility of distant objects: Journal of the Optical Society of America, **38**, 237–249.

Horvath, H., 1981, Atmospheric visibility: Atmospheric Environment, **15**, 1785-1796.

ICAO, 2004, Meteorological Service for International Air Navigation, Manual, Annex 3, 148 pp.

ICAO, 2005, Manual of Runway Visual Range Observing and Reporting Practices, Doc 9328, third edition, 105 pp.

Jenamani, R., and Tyagi, A., 2011, Monitoring fog at IGI airport and analysis of its runway-wise spatio-temporal variations using Meso-RVR network: Current Science, **100**(4), 491-501.

Kim, K. W., 2018, The comparison of visibility measurement between image-based visual range, human eye-based visual range, and meteorological optical range: Atmospheric Environment, **190**, 74-86.

Koschmieder, H., 1924, Theorie der horizontalen sichtweite: Beiträge zur Physik der freien Atmosphäre: Meteorologische Zeitschrift, **12**, 33–55.

Lee, Z., and Shang, S., 2016, Visibility: How applicable is the century-old Koschmieder model?: Journal of the Atmospheric Sciences, **73**, 4573-4581.

Liou, K. N., 2002, An introduction to at-

mospheric radiation, **84**: Elsevier.
Malm, W., 1999, Introduction to Visibility: Colorado State University, 79 pp.
Matsuzawa, M., and Takechi, H., 2012, Evaluating the degree of visibility deterioration perceived by drivers during snowstorms: SIRWEC, Helsinki, ID 37, 23-25 May 2012.
Meteo France, 2020, Visibility for Aeronautical Purposes: Report, 33 pp.
Middleton, W. E. K., 1947, Visibility in Meteorology: The Theory and Practice of the Measurement of the Visual Range: University of Toronto Press, 165 pp.
Middleton, W., 1952, Vision through the Atmosphere: University of Toronto Press.
Sabetghadam, S., Ahmadi-Givi, F., and Golestani, Y., 2014, Application of a digital image processing method for determination of atmospheric extinction coefficient for the city of Tehran: Geophysics, **9**(2), 40-51.
Stuke, S., 2016, Characterizing Thin Clouds Using Aerosol Optical Depth Information: University of Innsbruck.
Vaisala, 2011, Transmissometer Sensor LT31: Vaisala Manual, 292 pp.
WMO, 1990, The First WMO Intercomparison of Visibility Measurements: Report, 153 pp.
WMO, 2008, Guide to Meteorological Instruments and Methods of Observation: Guide 8, 681 pp.
Zege, E. P., Ivanov, A. P., and Katsev, I. L., 1991, Image Transfer through a Scattering Medium: Springer-Verlag.